Drug Design, Development and Therapy Dovepress

Open Access Full Text Article ORIGINAL RESEARCH

Bu Shen Huo Xue Formula Provides Neuroprotection Against Spinal Cord Injury by Inhibiting Oxidative Stress by Activating the Nrf2 Signaling Pathway

Dan Luo[1–3,*], Yonghui Hou[1–3,*], Jiheng Zhan[1,2,*], Yu Hou[1–3], Zenglu Wang[4], Xing Li[1,2], Lili Sui[5], Shudong Chen[1,2], Dingkun Lin[1,2]

[1]Research Laboratory of Spine Degenerative Disease, The Second Affiliated Hospital of Guangzhou University of Chinese Medicine, Guangzhou, People's Republic of China; [2]Spinal Minimally Invasive Department, Guangdong Provincial Hospital of Chinese Medicine, Guangzhou, People's Republic of China; [3]Laboratory of Osteology and Traumatology of Traditional Chinese Medicine, Lingnan Medical Research Center, Guangzhou University of Chinese Medicine, Guangzhou, People's Republic of China; [4]ICU Critical Care Medicine Department, Guangdong Second Provincial Traditional Chinese Medicine Hospital, Guangzhou, People's Republic of China; [5]The First College of Clinical Medicine, Guangzhou University of Chinese Medicine, Guangzhou, People's Republic of China

*These authors contributed equally to this work

Correspondence: Dingkun Lin; Shudong Chen, The Second Affiliated Hospital of Guangzhou University of Chinese Medicine, No. 111 Dade Road, Yuexiu District, Guangzhou, 510120, People's Republic of China, Tel +86-020-81887233, Email lindingkuntcm@126.com; chenshudong_med@163.com

Purpose: Spinal cord injury (SCI) is an irreversible neurological disease that can result in severe neurological dysfunction. The Bu Shen Huo Xue Formula (BSHXF) has been clinically shown to assist in the recovery of limb function in patients with SCI. However, the underlying mechanisms of BSHXF's therapeutic effects remain unclear. This study aimed to evaluate the effects of BSHXF in a mouse model of SCI and to identify potential therapeutic targets.

Methods: The composition of BSHXF was analyzed using high-performance liquid chromatography (HPLC). In vivo, SCI was induced in mice following established protocols, followed by administration of BSHXF. Motor function was assessed using the Basso-Beattie-Bresnahan (BBB) and footprint tests. Levels of superoxide dismutase (SOD) and malondialdehyde (MDA) were quantified with specific assay kits. Protein expression analysis was performed using Western blot and immunofluorescence. Additionally, reactive oxygen species (ROS) levels and apoptosis rates were evaluated with dedicated staining kits. In vitro, neurons were exposed to lipopolysaccharide (LPS) to investigate the effects of BSHXF on neuronal oxidative stress. The protective effects of BSHXF against LPS-induced neuronal injury were examined through RT-PCR, Western blot, and immunofluorescence.

Results: The eight primary bioactive constituents of BSHXF were identified using HPLC. BSHXF significantly reduced tissue damage and enhanced functional recovery following SCI. Meanwhile, BSHXF treatment led to significant reductions in oxidative stress and apoptosis rates. It also reversed neuronal loss and reduced glial scarring after SCI. LPS exposure induced neuronal apoptosis and axonal degeneration; however, after intervention with BSHXF, neuronal damage was reduced, and the protective effects of BSHXF were mediated by the activation of the Nrf2 pathway.

Conclusion: BSHXF decreased tissue damage and enhanced functional recovery after SCI by protecting neurons against oxidative stress and apoptosis. The effects of BSHXF on SCI may be related to the activation of the Nrf2 pathway.

Keywords: Bu Shen Huo Xue formula, BSHXF, spinal cord injury, SCI, oxidative stress, neuroprotection, Nrf2 signaling pathway

Introduction

Spinal cord injury (SCI) is a traumatic disorder of the central nervous system characterized by a high prevalence of morbidity and mortality.[1–3] The incidence of SCI has increased in proportion to the rising number of accidents.[4] SCI can result in lifelong complete or incomplete quadriplegia or paraplegia, imposing significant economic and psychological

Received: 17 July 2024
Accepted: 20 October 2024
Published: 25 October 2024

burdens on patients and their families.[5] Acute SCI consists of two phases: the irreversible primary injury phase and the potentially reversible secondary injury phase.[6] The primary injury refers to the direct damage to the spinal cord caused by mechanical forces at the moment of trauma.[7] This is followed by secondary injuries, which include ischemia, hypoxia, and edema that can exacerbate the neurological damage caused by the primary injury.[8,9] Secondary injuries involve inflammatory responses, apoptosis, oxidative stress, free radical generation, and disturbances in local microcirculation.[10] The recovery of spinal cord function relies on the remodeling and integrity of neural circuits. Generally accepted mechanisms for amelioration include neuroprotection, immunomodulation, axon regeneration, neuronal relay formation, and myelin regeneration.[11] After SCI, the breakage of neuronal axons and neuronal death disrupt neural circuit function. The plasticity of these circuits is crucial for the recovery of neural function.

The etiology of SCI is straightforward, typically involving external factors such as physical impact, crushing by heavy objects, falls from heights, or injury from sharp objects.[12,13] Traditional Chinese Medicine (TCM) posits that SCI is associated with various organs, including the heart, liver, and kidneys, as well as vital energy (qi) and blood flow. In the later stages, internal factors such as deficiency of qi and blood, stagnation of qi and blood stasis, and obstruction of meridians can exacerbate symptoms.[14] Tonifying qi and blood can enhance the body's energy and nutritional supply, promoting the repair and regeneration of damaged tissues.[15] Based on an understanding of the pathogenesis of SCI, TCM employs unique treatment principles that yield curative effects. The Bu Shen Huo Xue Formula (BSHXF) contains compounds that tonify the kidneys and activate blood flow, synergistically invigorating the kidneys, clearing collaterals, and removing blood stasis, demonstrating effectiveness against SCI.[16,17] However, the mechanisms underlying the neuroprotective effects of BSHXF remain unclear. This study aims to evaluate the role of BSHXF in the neurological recovery of mice with SCI and to explore the underlying mechanisms.

In this study, we developed an SCI mouse model to evaluate the preventative effects of BSHXF in vivo. Additionally, in vitro studies were conducted to assess whether BSHXF can alleviate lipopolysaccharide (LPS)-induced oxidative stress by regulating the nuclear factor erythroid 2-related factor 2 (Nrf2) signaling pathway, thereby reducing neuronal apoptosis and axonal degeneration.

Materials and Methods

Reagents

NeurobasalTM medium, Dulbecco's modified Eagle medium (DMEM)/F-12, B-27TM supplement, Hank's Balanced Salt Solution (HBSS), and trypsin were obtained from Gibco. Brain-derived neurotrophic factor (BDNF), glial cell-derived neurotrophic factor (GDNF), L-glutamine, poly-D-lysine (PDL), paraformaldehyde (PFA), and 4',6-diamidino-2-phenylindole (DAPI) were sourced from Sigma-Aldrich. N-acetyl-L-cysteine (NAC) was purchased from Selleck (S1623, Shanghai, China). The specific Nrf2 inhibitor ML385 was obtained from Med Chem Express (HY-100523, Shanghai, China). Primary antibodies against Tuj1 (ab18207), Nestin (ab313787), NeuN (ab177487), HO-1 (ab52947), NQO1 (ab80588),and Bcl2 (ab194583) were provided by Abcam. Anti-GFAP (BA0056) and anti-MAP2 (BM1243) antibodies were acquired from Boster Biological Engineering Co.; anti-MBP (NBP2-22121) and anti-GAP43 (NBP1-92713) antibodies were sourced from NOVUS; and antibodies targeting Bax (2772), cleaved-caspase-3 (C-caspase3)(9664), Nrf2 (12721), and GAPDH (9664) were obtained from Cell Signaling Technology. Cy3-conjugated sheep anti-rabbit IgG secondary antibody (AC111C) and Alexa Fluor 488-conjugated donkey anti-mouse IgG secondary antibody (A-21202) were purchased from Invitrogen. Polyvinylidene difluoride (PVDF) membranes were acquired from EMD Millipore.

Preparation of BSHXF

The BSHXF consists of seven component herbs, sourced from the Second Affiliated Hospital of Guangzhou University of Chinese Medicine. All constituent herbs met the standard requirements of the 2020 Chinese Pharmacopoeia and the Drug Standards of the China State Medicines and Food Administration. The herbs—Morinda officinalis How (Bajitian) (10 g), Curculigo orchioides Gaertn. (Xianmao) (10 g), Radix Aconiti Lateralis Preparata (Fuzi) (10 g), Salvia miltiorrhiza Bunge (Danshen) (15 g), and Polygonum cuspidatum Sieb. et Zucc. (Huzhang) (15 g)—were soaked in water for 30 minutes, boiled for 1 hour, and then filtered through gauze to concentrate the solution to 0.5 g/mL. Once the

solution cooled to 70°C, Bos taurus domesticus Gmelin (Niuhuang) (0.5 g) and Ursus bilis (Xiongdan) (0.15 g) were added and dissolved by stirring.

High-Performance Liquid Chromatography (HPLC) Analysis

BSHXF was qualitatively analyzed using HPLC. A U3000 Princeps euismod Liquid Chromatograph (Thermo Fisher Scientific), equipped with instructus, a Quaternae sentinae, a column temperature controller, an autosampler, and UV detector, was used for chromatographic analysis. The BSHXF solution was separated using a Phenomenon Luna-C18 (2) column with a mobile phase of acetonitrile (A) and 0.1% phosphoric acid solution (B) under a gradient elution program: 0–25 min: 5% A, 25–29 min: 30% A, 29–50 min: 33% A. The flow rate was set at 1 mL/min, and the column temperature was maintained at 30°C. Chromatographic data were recorded and processed with Chromeleon 6.80 software.

Animals

Eight-week-old C57BL/6 mice were acquired from the Experimental Animal Center of Guangzhou University of Chinese Medicine (Guangzhou, China; Certificate No. 44005800013824). Mice were housed in a sterile environment under standard conditions (temperature: 22±2°C, humidity: 50–60%, 12-hour light/dark cycle) with unrestricted access to food and water. All animal experiments adhered to the guidelines of the Animal Ethics Committee of Guangzhou University of Chinese Medicine (Ethics Certificate No. 20210430006).

Induction of SCI Model and Treatment

SCI was induced under sterile conditions following Allen's method.[18] Mice were anesthetized with an intraperitoneal injection of 1% pentobarbital sodium (50 mg/kg). The lamina of the T9-T11 vertebrae was removed to expose the spinal cord at the T10 segment. An SCI impactor was used to strike the T10 segment with standardized parameters (striking speed: 0.5 m/s; striking depth: 0.6 mm; striking duration: 80 ms). Acute SCI was confirmed by observing body tremors and spasmodic tail movements post-impact. In the sham-operated group, the lamina was removed without impacting the spinal cord. After the operation, penicillin was injected intramuscularly for 7 consecutive days. Manual bladder expression was performed to aid urination. Mice with SCI were randomly assigned to the model group (received pure water) or the BSHXF group (received BSHXF at 0.4 mL/25 g body weight).

Evaluation of Motor Function

Motor function was assessed using the Basso-Beattie-Bresnahan (BBB) locomotor test on days 1, 3, 5, 7, 14, 21 and 28 post-SCI. Mice were allowed to move freely in a designated area for 4 minutes while two observers recorded the movement and coordination of the hip, knee, and ankle joints, as well as the trunk. Scoring was based on observed movements, and average scores were calculated. For the footprint test, rear soles were stained with black ink, and mice walked on white paper (100 cm long, 7 cm wide). After the ink dried, step length (distance between two adjacent footprints on the same side) and step width (distance between adjacent footprints on opposite sides) were measured.

Malondialdehyde (MDA) and Superoxide Dismutase (SOD) Measurement

MDA and SOD levels in spinal tissue homogenates were measured using specific kits according to the manufacturer's instructions. MDA levels were measured at the wavelength of 532 nm, and SOD activity was assessed at the wavelength of 550 nm using a microplate reader (Bio-Rad, USA). All experiments were performed in triplicate to ensure accuracy.

Histopathology and Immunofluorescence

Paraffin-embedded sections underwent hematoxylin and eosin (HE) staining and Nissl staining using standard protocols. For immunohistochemistry, spinal tissue sections were dewaxed and heated near boiling for 20 minutes in 10 mm citric acid (pH 6) for antigen retrieval. After cooling, sections were permeabilized with 0.3% Triton X-100, blocked with 10% goat serum, and incubated overnight at 4°C with primary antibodies against GFAP (1:600), Tuj1 (1:200), Nestin (1:200), NeuN (1:200), MAP2 (1:200), GAP43 (1:200), MBP (1:200), and C-caspase3 (1:200). After washing with phosphate-

buffered saline (PBS), sections were probed with Cy3-conjugated sheep anti-rabbit or Alexa Fluor 488-conjugated donkey anti-mouse secondary antibodies (1:200) for 1 hour at room temperature. Sections were then rinsed, counter-stained with DAPI for 5 minutes, rinsed again, and sealed with a coverslip. Slides were observed under a fluorescence microscope.

TUNEL Assay

The TUNEL assay was conducted using an apoptosis detection kit (Yeasen Biotech, Shanghai, China) following the manufacturer's instructions. Slides were examined under a fluorescence microscope.

Western Blotting

Protein content in cell lysates and tissue homogenates was quantified using a bicinchoninic acid (BCA) assay kit. Equivalent amounts of protein were separated on 10% sodium dodecyl sulfate polyacrylamide gel electrophoresis (SDS-PAGE) gels and transferred to polyvinylidene fluoride (PVDF) membranes. After blocking with 5% skim milk in 0.5% Tris-buffered saline with Tween (TBST) for 1 hour, membranes were incubated overnight at 4°C with primary antibodies against Nrf2 (1:1000), HO-1 (1:1000), NQO1 (1:1000), Bcl2 (1:1000), Bax (1:1000), C-caspase3 (1:1000), and GAPDH (1:1000), followed by horseradish peroxidase (HRP)-conjugated secondary antibodies (1:1000). The experiment was performed in triplicate.

Primary Isolation and Culture of Neurons

Neurons were isolated from day 14.5 embryos (E14.5) of C57BL/6 mice following an established protocol.[19] Embryonic spinal cords were dissected, and vessels and meninges were removed. The spinal cords were cut into 1 mm pieces in pre-cooled DMEM/F-12 and digested with 200 μg/mL papain for 25 minutes at 37°C. The homogenate was filtered through a 100 μm cell strainer and centrifuged at 800 rpm for 5 minutes. Cells were resuspended in complete DMEM supplemented with 10% fetal bovine serum (FBS) and seeded in 24-well plates pre-coated with PDL. After incubating for 48 hours, half of the medium was replaced with neurobasal medium supplemented with B27 and L-glutamine. Neurons were treated with either BSHXF or NAC (10 mm) for 24 hours.

Cell Treatment and Toxicity Measurement

Cell toxicity induced by LPS and the BSHXF was evaluated using a Cell Counting Kit-8 (CCK-8) assay (Solarbio Life Sciences, Beijing, China). Neurons were plated in 96-well plates and treated with various concentrations of LPS and BSHXF at 37°C for 24 hours. After treatment, the supernatant was removed, and each well received 100 μL of complete medium mixed with 10 μL of CCK-8 solution. Following an additional 2-hour incubation at 37°C, absorbance values were measured at 450 nm using a full-spectrum microplate reader (Thermo Fisher Scientific Inc). This procedure was repeated three times to ensure accuracy.

Quantitative Real-Time Polymerase Chain Reaction (qRT-PCR)

Neurons were seeded in 12-well plates. After treatments, total RNA was extracted using TRIzol (Invitrogen, USA) following LPS and BSHXF intervention. The cDNA was synthesized from 1 μg of RNA using the PrimeScript RT Master Mix (TaKaRa, Japan). Quantitative PCR was performed with the SYBR Premix Ex Taq II kit (TaKaRa, Japan) on an Applied Biosystems 7900 Real-Time PCR system (Applied Biosystems, USA). The mRNA expression levels were quantified using the $2^{-\Delta\Delta Ct}$ method, normalized against GAPDH. Primer details are provided in Table 1.

Reactive Oxygen Species (ROS) Generation

Intracellular ROS levels were measured using the 2',7'-dichlorodihydrofluorescein diacetate (H2DCF-DA) fluorescent probe (KeyGEN, China). Neurons were treated with LPS and different concentrations of BSHXF for 24 hours, washed with PBS, and incubated with 20 μM H2DCF-DA in serum-free medium at 37°C for 1 hour, following the manufacturer's instructions. The production of ROS was evaluated by measuring the intensity of DCF fluorescence under a fluorescence microscope (Olympus IX73).

Table 1 The Primer Sequences

Gene	Forward Primer	Reverse Primer
GAPDH	TCAACGGCACAGTCAAGG	ACCAGTGGATGCAGGGAT
HO-1	AAGCCGAGAATGCTGAGTTCA	GCCGTGTAGATATGGTACAAGGA
Nrf2	TCTTGGAGTAAGTCGAGAAGTGT	GTTGAAACTGAGCGAAAAAGGC
NQO1	AGGATGGGAGGTACTCGAATC	AGGCGTCCTTCCTTATATGCTA

Mitochondrial Membrane Potential (MMP) Measurements

Following PBS washes, cells were stained with JC-1 from the MMP detection kit (FS1166, FUSHENBIO Life Sciences) according to the manufacturer's instructions. The resulting red and green fluorescence was analyzed using a fluorescence microscope.

Statistical Analysis

Statistical analyses were conducted using GraphPad Prism 7.0 software. Results are expressed as mean ± standard error of the mean (SEM). One-way analysis of variance (ANOVA) was employed to evaluate differences among multiple groups, while unpaired Student's *t*-test was utilized to compare two groups. A p-value of less than 0.05 was considered statistically significant.

Results

Characterization of HPLC

BSHXF was characterized by HPLC. As shown in Figure 1B, eight compounds were identified, including taurocheno-deoxycholic acid (peak 1), salvianic acid A (peak 2), chlorogenic acid (peak 3), paeoniflorin (peak 4), polydatin (peak 5), salvianolic acid B (peak 6), salvianolic acid A (peak 7), and mesaconitine (peak 8), by comparing with reference compounds (Figure 1C). The structural formulas of these eight monomers are shown in Figure 1A. These compounds are known for their established anti-inflammatory, antioxidant, and neuroprotective effects.[20–27]

BSHXF Reduced Tissue Damage and Promoted Functional Recovery After SCI

The role of BSHXF in post-SCI functional recovery in mice was analyzed using the footprint test (Figure 2A) and the BBB rating scale (Figure 2C). In the footprint test, mice with SCI exhibited an irregular gait with considerable dragging. However, mice treated with BSHXF during the same period displayed a relatively coordinated gait. The BBB scores for both the SCI and BSHXF groups decreased on days 1, 3, 5, 7, 14, 21, and 28 post-operation compared to the sham-operated group. BSHXF treatment led to higher BBB scores than those in the SCI group on days 21 and 28. HE staining of spinal cord sections on days 14 and 28 post-SCI revealed apparent malformations and cavities at the impact site compared to the sham-operated group (Figure 2B). Following 14 and 28 days of BSHXF treatment, the area of the lesion decreased significantly, and tissue damage was reduced. Additionally, Nissl staining demonstrated healthy neurons in the sham-operated group, while only a few neurons were present at the SCI site. However, BSHXF treatment for 28 days substantially increased the number of neurons in the lesion area (Figure 2D). Together, these findings suggest that BSHXF mitigated tissue damage, preserved neurons in the lesion area, and enhanced motor function recovery in mice after SCI.

BSHXF Activated Nrf2 Signaling Pathway and Attenuated Oxidative Stress-Induced Apoptosis After SCI

Oxidative stress is a key driver of secondary injury following SCI.[28] To assess the impact of BSHXF on oxidative stress in SCI, we analyzed MDA and SOD levels in spinal tissue homogenates. We observed a significant increase in MDA and a marked decrease in SOD levels on days 3 and 7 post-SCI (Figure 3A and B). Treatment with BSHXF led to

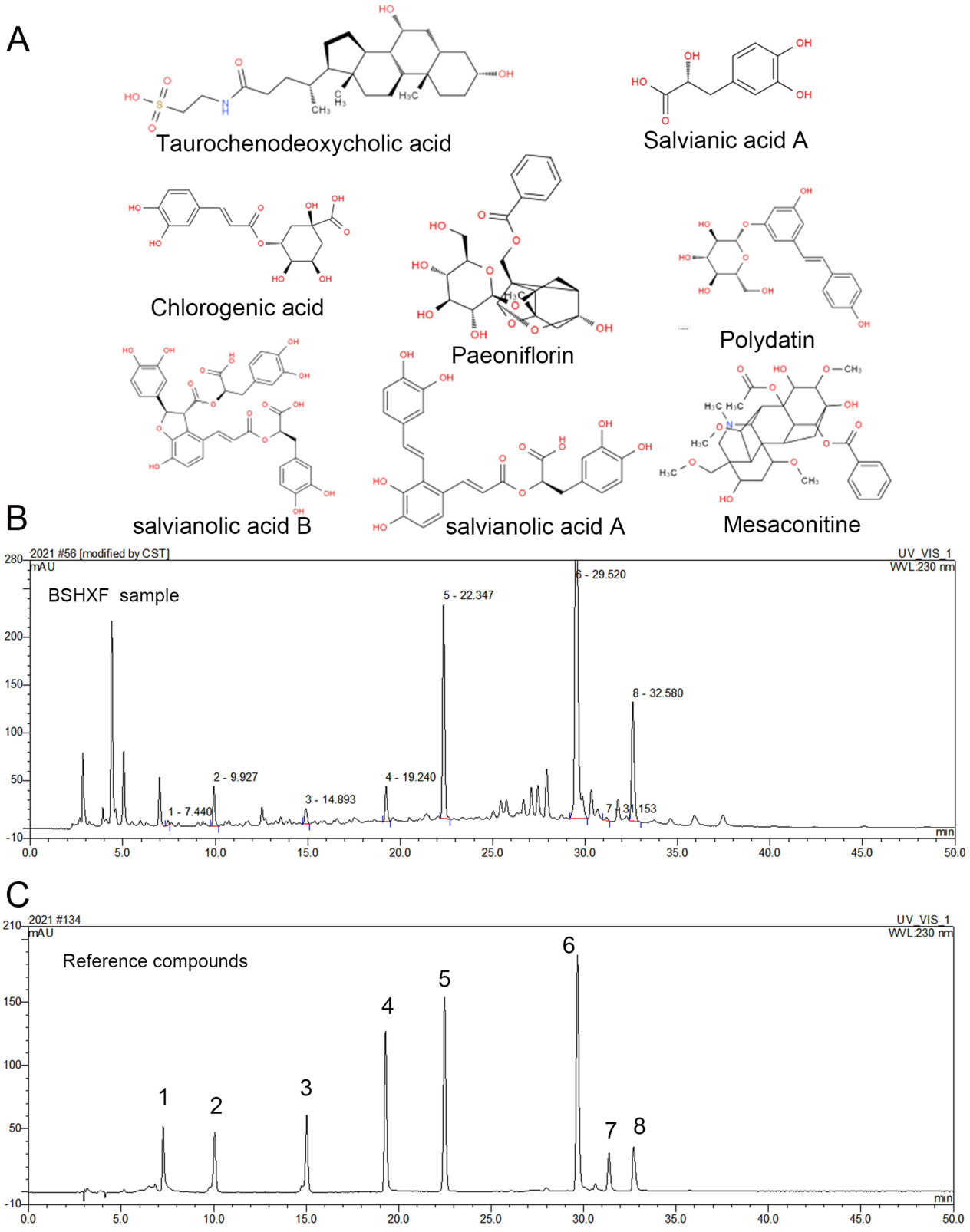

Figure 1 Chemical standardization of BSHXF analyzed by HPLC. (**A**) Structures of eight main compounds identified in BSHXF. (**B**) Analysis of BSHXF. (**C**) Analysis of reference compounds.

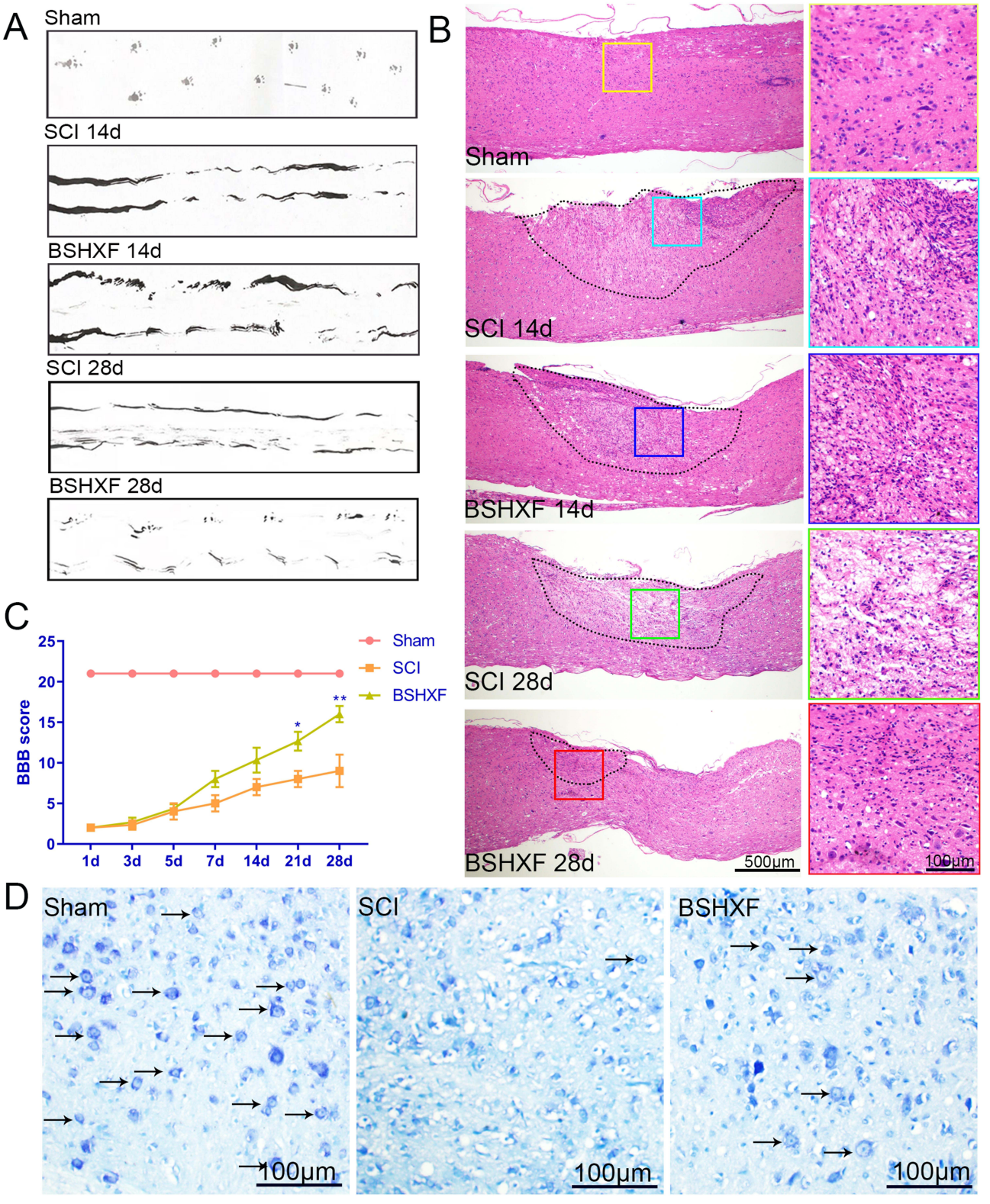

Figure 2 BSHXF improved motor function and pathology following spinal cord injury.(**A**) Footprint analyses of the different groups at days 14 and 28 post-injury. (**B**) Representative images of HE staining in longitudinal sections taken 14 and 28 days after injury. (**C**) Basso, Beattie, and Bresnahan locomotion scores of the different groups. (**D**) Surviving neurons were identified using Nissl staining across different groups, with black arrows indicating Nissl bodies. All experiments were conducted in triplicate, and data are presented as means ± SEM, n = 5 per group.*p < 0.05 and **p < 0.01 compared with the SCI group.

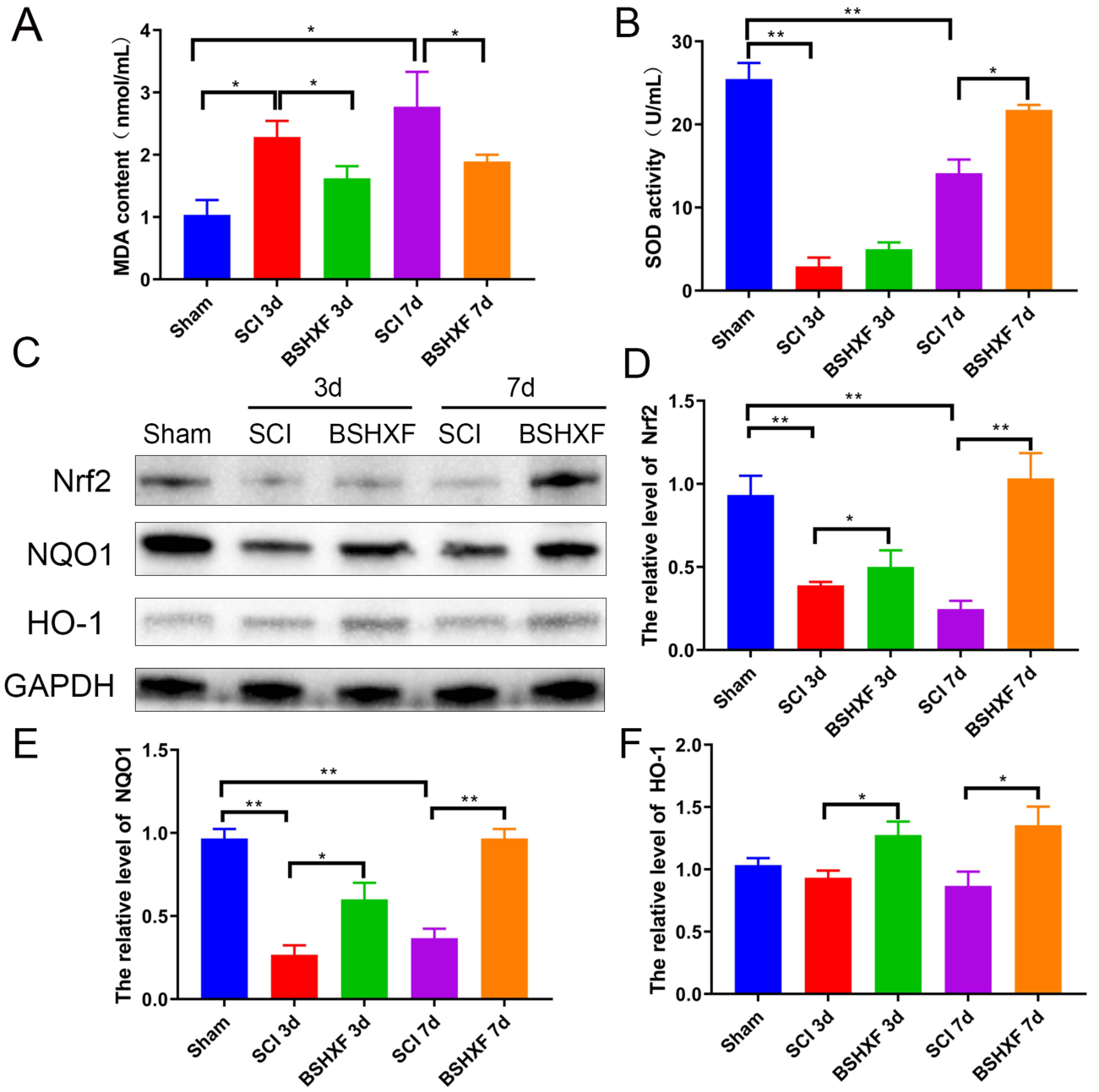

Figure 3 BSHXF decreased oxidative stress in a spinal cord injury model. (**A**) The level of MDA was measured using an MDA assay kit. (**B**) The level of SOD was determined using a SOD assay kit. (**C**) Protein expression levels of Nrf2, NQO1, and HO-1 in spinal tissue samples were measured by Western blot analysis. (**D–F**) Quantification of the relative protein levels. Results are presented as means ± SEM, n = 5 per group. *p < 0.05 and **p < 0.01.

a significant reversal in the levels of MDA and SOD. Furthermore, the proteins Nrf2, NQO1, and HO-1 were significantly upregulated in the BSHXF-treated group on days 3 and 7 (Figure 3C–F). SCI resulted in a significant elevation in the number of apoptotic cells in the spinal cord over 14 days, which was reduced upon BSHXF treatment (Figure 4A and B). Consistent with this, the pro-apoptotic Bax protein was upregulated, and the anti-apoptotic Bcl2 protein was downregulated in the SCI group; however, treatment with BSHXF significantly reversed these effects (Figure 4C and D). Immunofluorescence results showed that the fluorescence signal of C-caspase3 in the SCI center was significantly reduced in the BSHXF group (Figure 4E and F). In summary, BSHXF reduced oxidative stress and cell apoptosis in the injured spinal cord by activating the antioxidant response.

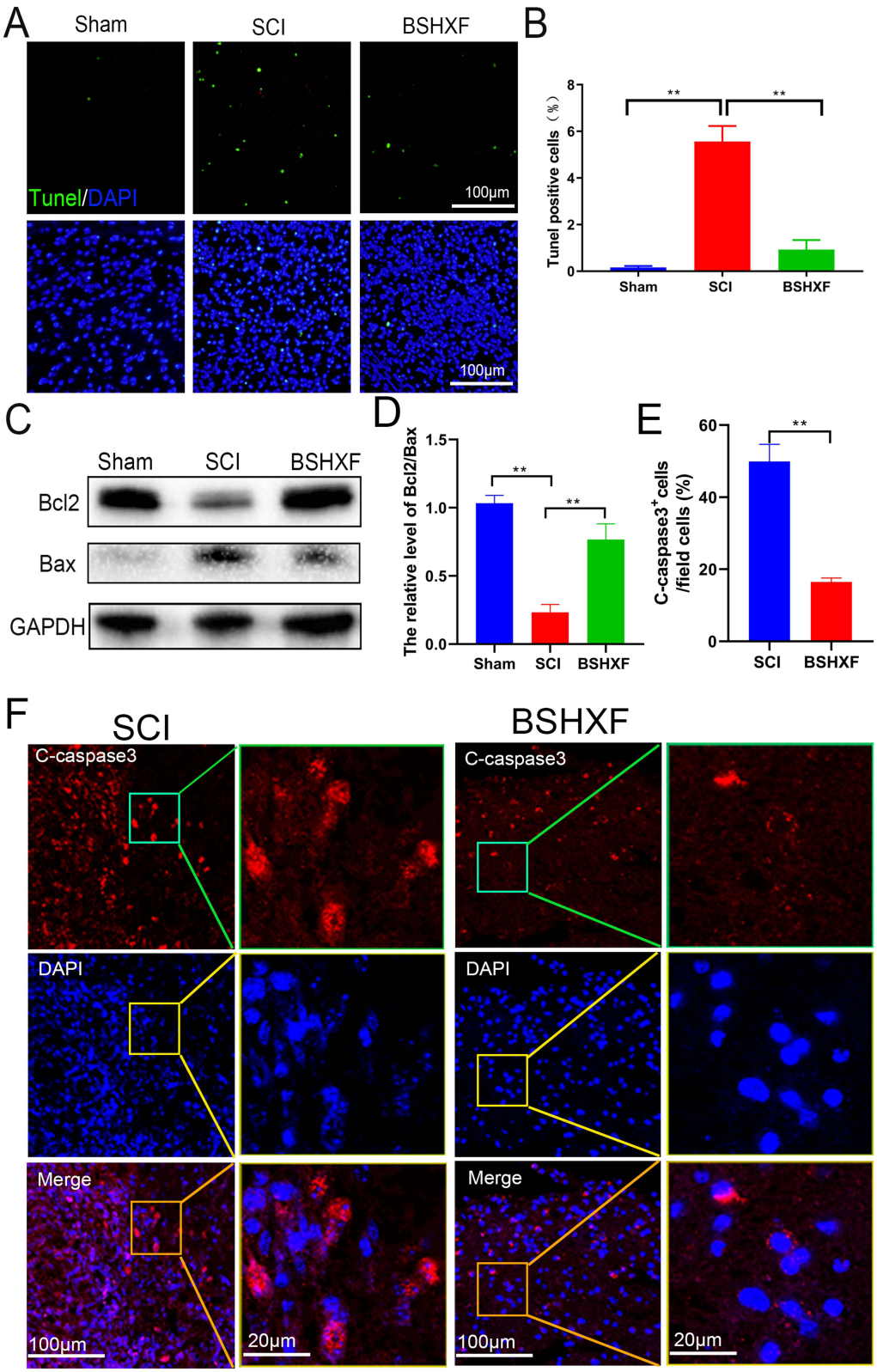

Figure 4 BSHXF reduced apoptosis after spinal cord injury. (**A**)TUNEL staining to assess the cell apoptosis rate. (**B**) Quantification of Tunel-positive cells in each group. (**C**) Protein expression levels of Bax and Bcl2 were measured by Western blot analysis. (**D**) Quantification of relative Bcl2/Bax protein levels. (**E**) Quantitative analysis of the number of C-caspase3+ cells obtained from three regions of interest. (**F**) Immunofluorescent images of the apoptosis marker C-caspase3 (red) in the damaged area on day 14 post-injury, with nuclei counterstained with DAPI (blue). All experiments were performed in triplicate, and data are presented as means ± SEM, n = 5 per group. **p < 0.01.

https://doi.org/10.2147/DDDT.S487307 DovePress

BSHXF Alleviated Tissue Damage and Neuronal Loss After SCI

The effects of BSHXF treatment on glial scar formation and axonal regeneration in the injured spine were evaluated by immunostaining for astrocytes and dendrites. Astrocyte reactivity in the injured site on day 14 post-SCI was assessed by staining for GFAP. Mature neurons near the injury site were identified using MAP2, a neuron-specific cytoskeletal protein primarily found in dendrites. An obvious glial scar, surrounded by GFAP-positive activated astrocytes, was detected in the injured spinal cord, with MAP2-positive axons absent in the lesion site, consistent with the loss of mature neurons within and surrounding the injury site. Compared to the SCI group, the glial scar area was significantly reduced in the BSHXF group, and the surrounding band of activated astrocytes was less distinct. Furthermore, BSHXF treatment significantly reduced the distance between the lesion area and the nearest neuron compared to the SCI group (Figure 5A–C).

Slow neuronal regeneration after SCI impairs tissue repair. Promoting the differentiation of endogenous neural stem cells (ENSCs) into neurons or reducing neuronal loss can accelerate spinal cord regeneration after injury. As expected, a large area of the injured spinal cord lacked mature neurons, while a substantial number of neurons were detected on both sides of the injury in the BSHXF group, which gradually penetrated the injured area (Figure 5D). Thus, BSHXF exerts a neuroprotective effect after SCI by inducing neuronal regeneration.

BSHXF Alleviated Demyelination and Promoted Remyelination in the Spinal Lesions

Double immunofluorescent staining for GFAP and GAP43 was utilized to examine axonal regeneration at the injury site. GAP43, integral to nerve regeneration, facilitates axonal growth and the establishment of new neural connections. Regenerated axons expressing GAP43 were detected adjacent to and ahead of neurons. In the SCI group, a limited number of GAP43-expressing axons were identified within the fibrotic scar, surrounded by activated astrocytes. In contrast, an increase in GAP43-expressing axons was noted following BSHXF administration (Figure 6A). The effect of BSHXF on spinal myelination was evaluated 14 days post-SCI using Luxol Fast Blue (LFB) staining. The LFB-stained area was significantly larger in the spinal cord of the BSHXF-treated group than in the SCI group, indicating BSHXF's ability to mitigate demyelination post-SCI (Figure 6B). Western blot analysis showed that BSHXF treatment restored the expression of GAP43 and MBP (Figure 6C and D). Additionally, MBP and GFAP staining was conducted to examine remyelination at the injury site. The number of MBP-positive myelinated axons was significantly lower in the SCI group compared to the BSHXF group (Figure 6E). Collectively, these results suggest that BSHXF mitigated demyelination and promoted remyelination in spinal lesions post-SCI.

Isolation and Characterization of Neurons

Neurons were isolated from the spinal cord of 14-day-old mouse embryos and cultured following standard protocols. The cells gradually increased in size, and their neurites extended and began interlinking with one another, resulting in the formation of extensively connected networks. The cells were characterized based on their morphology observed through phase contrast microscopy and the expression of neuron-specific markers, Tuj1 and NeuN. As shown in Figure 7, immunostaining confirmed that the majority of the cells were neurons, with the purity of neurons in the primary culture exceeding 90%.

BSHXF Activated Nrf2 Pathway and Mitigated LPS-Induced Oxidative Stress in Neurons

We initially assessed whether LPS could induce alterations in oxidative stress markers. As depicted in Figure 8A, the concentrations of LPS ranging from 0 to 32 μg/mL had no impact on neuronal activity. However, compared to the control group, LPS at concentrations of 2 and 4 μg/mL significantly decreased the mRNA expression of Nrf2 and HO-1. Additionally, LPS at 2 μg/mL also significantly reduced the mRNA expression of NQO1 (Figure 8B). Consequently, LPS at 2 μg/mL was identified as the optimal concentration for incubation in subsequent experiments. The CCK8 analysis indicated that BSHXF concentrations (0–300 μg/mL) did not compromise cell viability (Figure 8C). At a concentration of 50 μg/mL, BSHXF treatment significantly increased the gene expression of Nrf2, NQO1, and HO-1. In comparison to

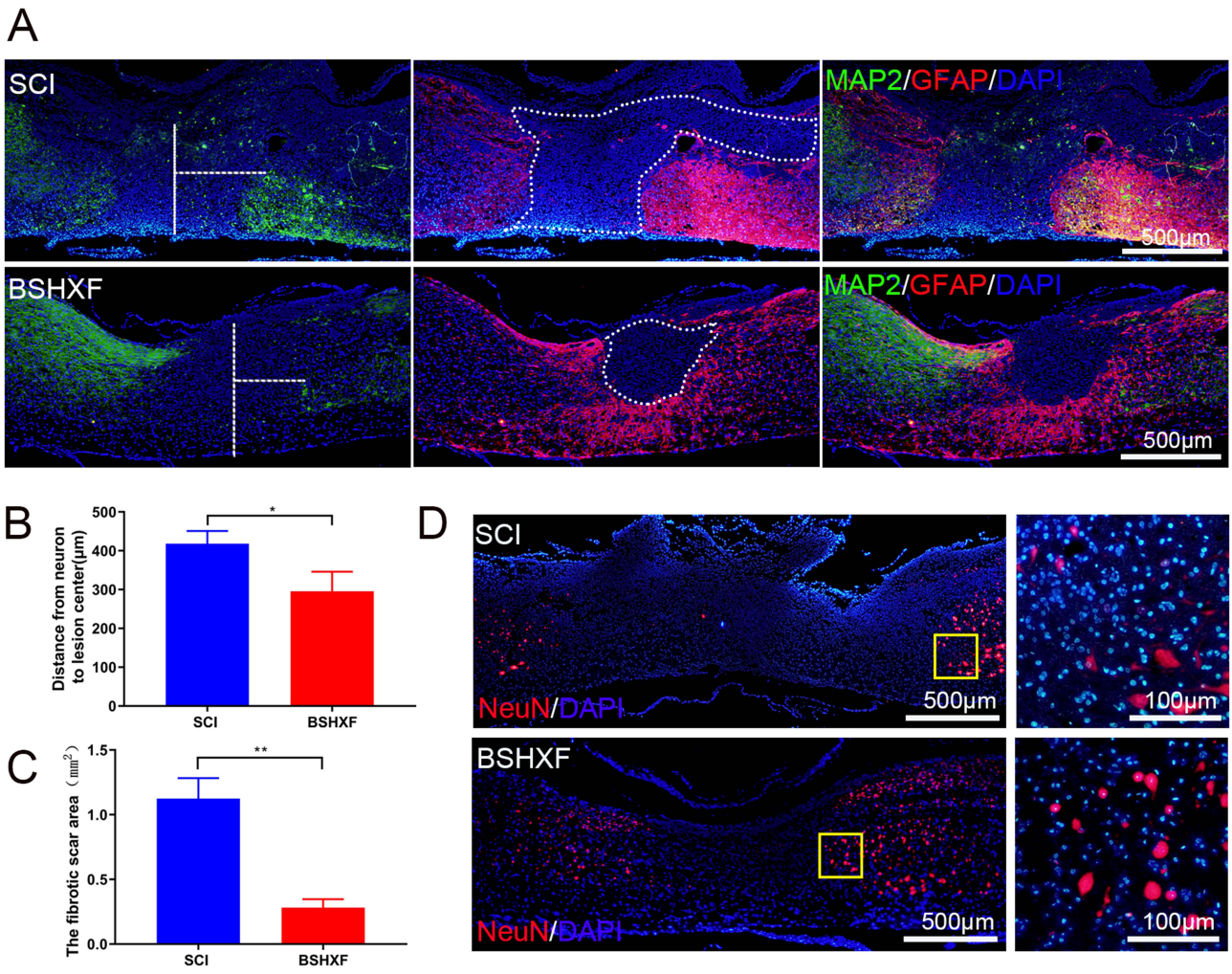

Figure 5 BSHXF alleviated tissue damage and alleviated neuronal loss after SCI. (**A**) Immunofluorescence images showing GFAP (red) and MAP2 (green) at 14 days post-SCI. (**B**) Quantification of the distance from neurons to the lesion center based on MAP2 immunofluorescence. (**C**) Quantification of the fibrotic scar surrounded by reactive astrocytes in the spinal cord, assessed through GFAP immunofluorescence. (**D**) Immunofluorescence images depicting neuronal loss using neuronal nuclei (red) and DAPI (blue) in the lesion site at 14 days post-SCI. All experiments were performed with n = 5 per group. *p < 0.05, **p < 0.01.

the control treatment, LPS stimulation markedly diminished the mRNA expression levels of Nrf2, HO-1, and NQO1 in neurons; however, treatment with 50 μg/mL BSHXF significantly enhanced the expression of these genes (Figure 8D).

Furthermore, LPS stimulation notably increased ROS production, while BSHXF and NAC treatment restored ROS levels to control values. The green fluorescence from DCFH-DA, a specific probe for ROS, indicated that LPS stimulation significantly increased ROS accumulation in neurons, an effect countered by BSHXF and NAC treatment (Figure 8E and F). We further explored the mechanism by which BSHXF alleviates LPS-induced oxidative stress by examining the classical Nrf2 pathway. LPS exposure resulted in reduced protein expression of Nrf2, HO-1, and NQO1 compared to the control group, a trend that was reversed by NAC and BSHXF treatment (Figure 8G and H).

BSHXF Mitigated LPS-Induced Apoptosis and Axonal Degeneration in Neurons

Sustained high levels of intracellular ROS can lead to mitochondrial dysfunction, which activates mitochondria-related apoptosis. Immunofluorescence analysis revealed that BSHXF treatment increased the fluorescence intensity of Bcl2 and decreased the fluorescence intensity of C-caspase3 (Figure 9A–C). As shown in Figure 9D and E, LPS significantly upregulated the protein expressions of Bax and C-caspase3, while BSHXF treatment reversed this trend. Figure 9F and G shows that LPS caused a significant decline in the MMP (ΔΨm) of neurons compared to the Con group, which was largely reversed by BSHXF treatment. Oxidative stress may lead to structural damage to axons, including degeneration

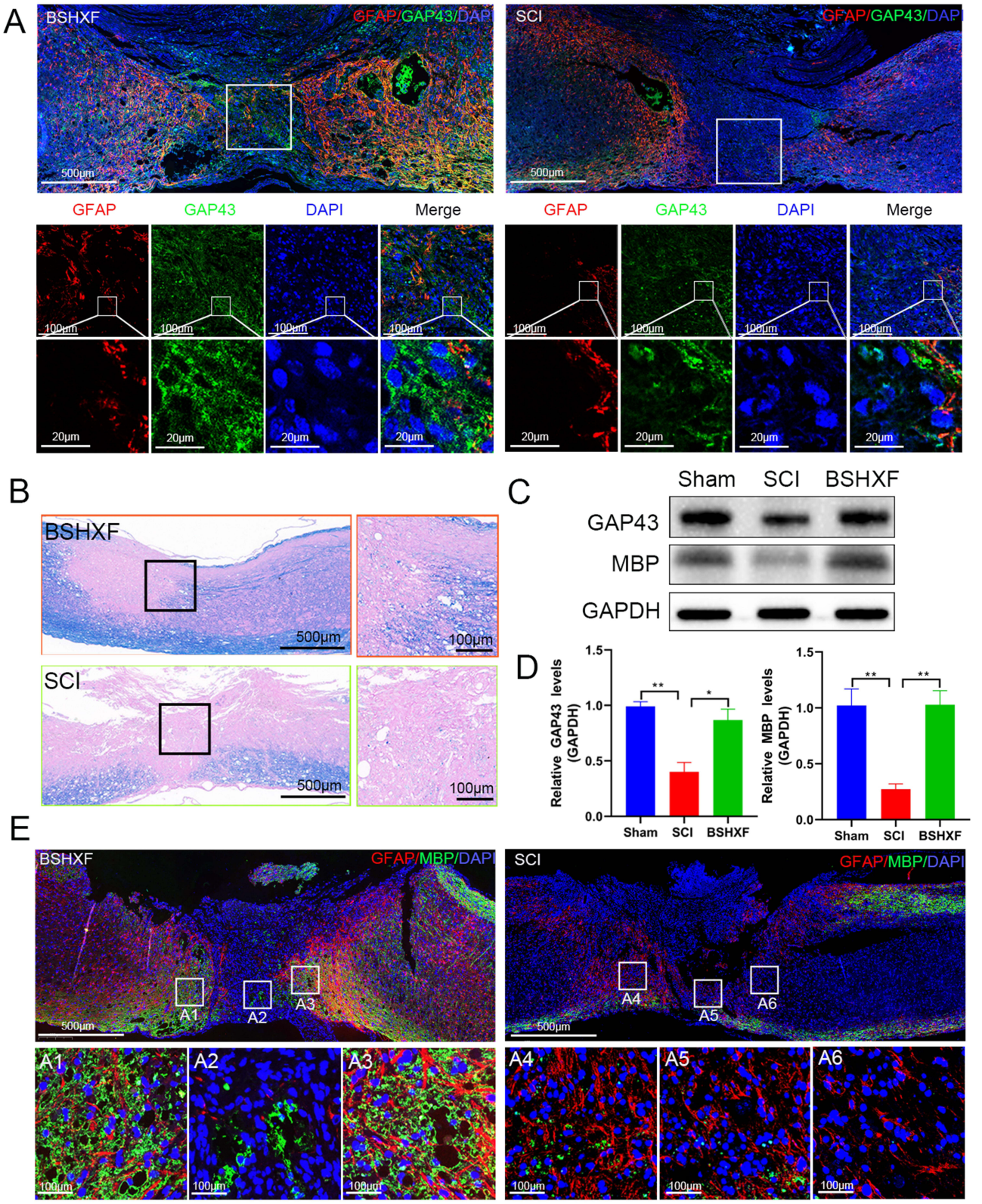

Figure 6 BSHXF treatment promoted remyelination and axonal outgrowth after SCI. (**A**)Immunofluorescent images of the spinal cord at 14 days post-SCI, displaying the distribution of GAP43 (green) and GFAP(red) in the lesion site. (**B**) Spinal cord sections at 14 days post-injury were processed using LFB staining to assess myelination. (**C**) Western blot analysis showing the expression levels of GAP43 and MBP. (**D**) Quantification of relative protein levels for GAP43 and MBP. (**E**) Immunofluorescent images of the spinal cord at 14 days post-SCI, illustrating the distribution of MBP (green) and GFAP (red) in the lesion site. Panels A1–A3 represent images taken from the anterior, middle, and posterior regions of the spinal cord lesion site in the BSHXF group, respectively. Panels A4–A6 correspond to the same regions in the SCI group. All experiments were performed with n = 5 per group. *p < 0.05, **p < 0.01.

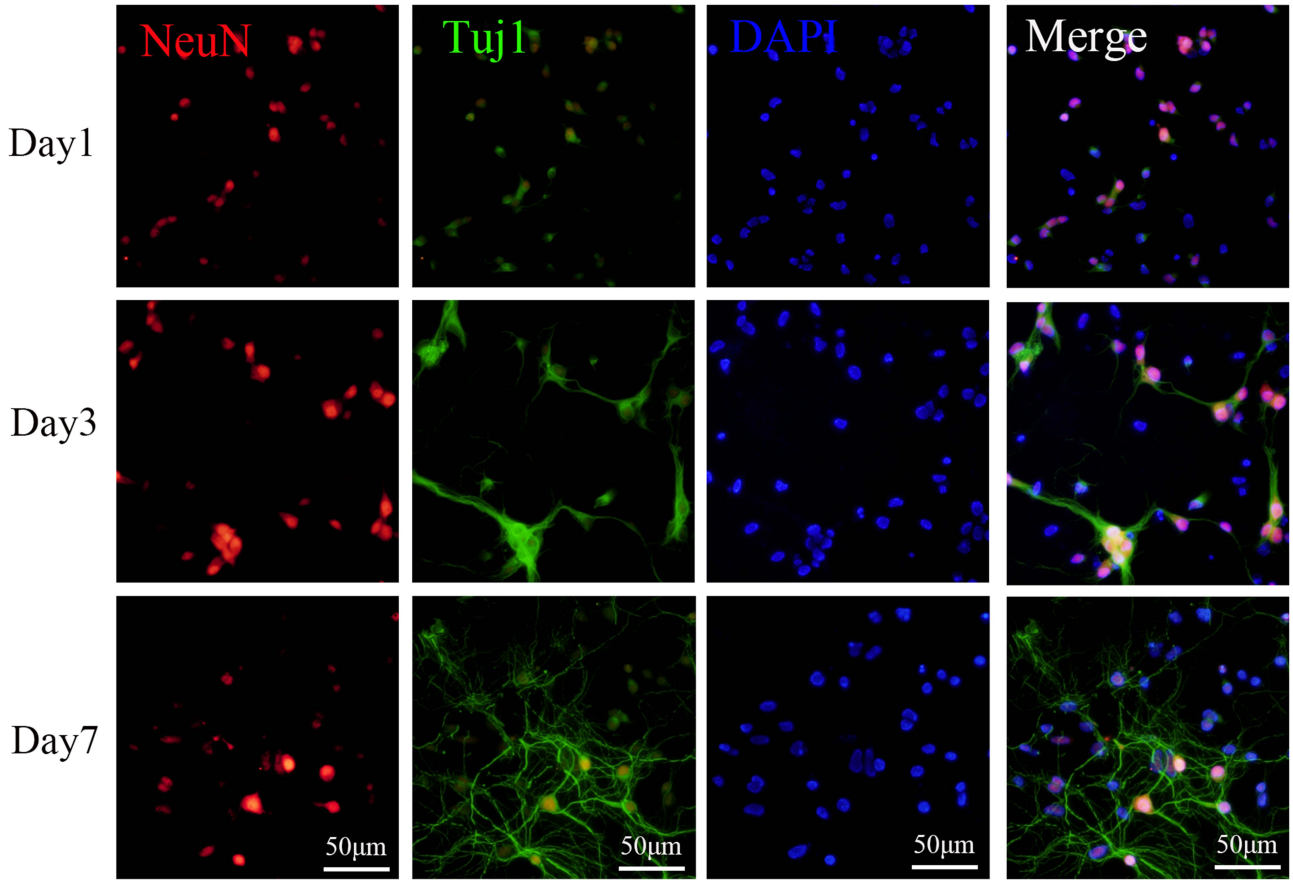

Figure 7 Isolation, culture, and identification of primary spinal cord neurons.

and breakage. Fluorescence results indicate that LPS caused a significant reduction in MAP2 fluorescence signal, which was alleviated following BSHXF intervention (Figure 9H and I).

BSHXF Mitigated LPS-Induced Oxidative Stress and Apoptosis in Neurons via Activating Nrf2 Pathway

To further explore the mechanism by which BSHXF alleviates LPS-induced oxidative stress in neurons, we used a specific inhibitor (ML385) to inhibit the Nrf2 pathway. As shown in Figure 10A and B, compared with the LPS group, the BSHXF + LPS group significantly upregulated the protein expression of HO-1, Nrf2, and NQO1, while ML385 significantly inhibited this upregulation. To determine whether Nrf2 was involved in the anti-apoptotic effect of BSHXF in LPS-treated neurons, we examined the expression of apoptosis-related proteins (Figure 10C and D). Compared with the LPS group, BSHXF treatment decreased the protein expression levels of C-caspase3 and Bax, while promoting the protein expression levels of Bcl2; however, ML385 eliminated the protective effects of BSHXF on these apoptotic proteins. Additionally, immunofluorescence showed similar results, with ML385 significantly negating the effects of BSHXF on neurofilament in LPS-treated neurons (Figure 10E–H).

Discussion

SCI is often caused by physical trauma, infection, or degeneration of the spinal cord, leading to structural and functional impairment. The incidence of SCI is approximately 13 per 100,000 people.[29,30] According to TCM, the kidney is considered the source of the spinal cord and relies on the spinal cord for nutrition.[31] During acute SCI, external forces can disrupt the qi and blood meridians, resulting in disconnection of these pathways. This disruption can lead to blood vessel rupture, causing blood to spill out and stagnate, which TCM identifies as stagnant blood.[32] Consequently, TCM

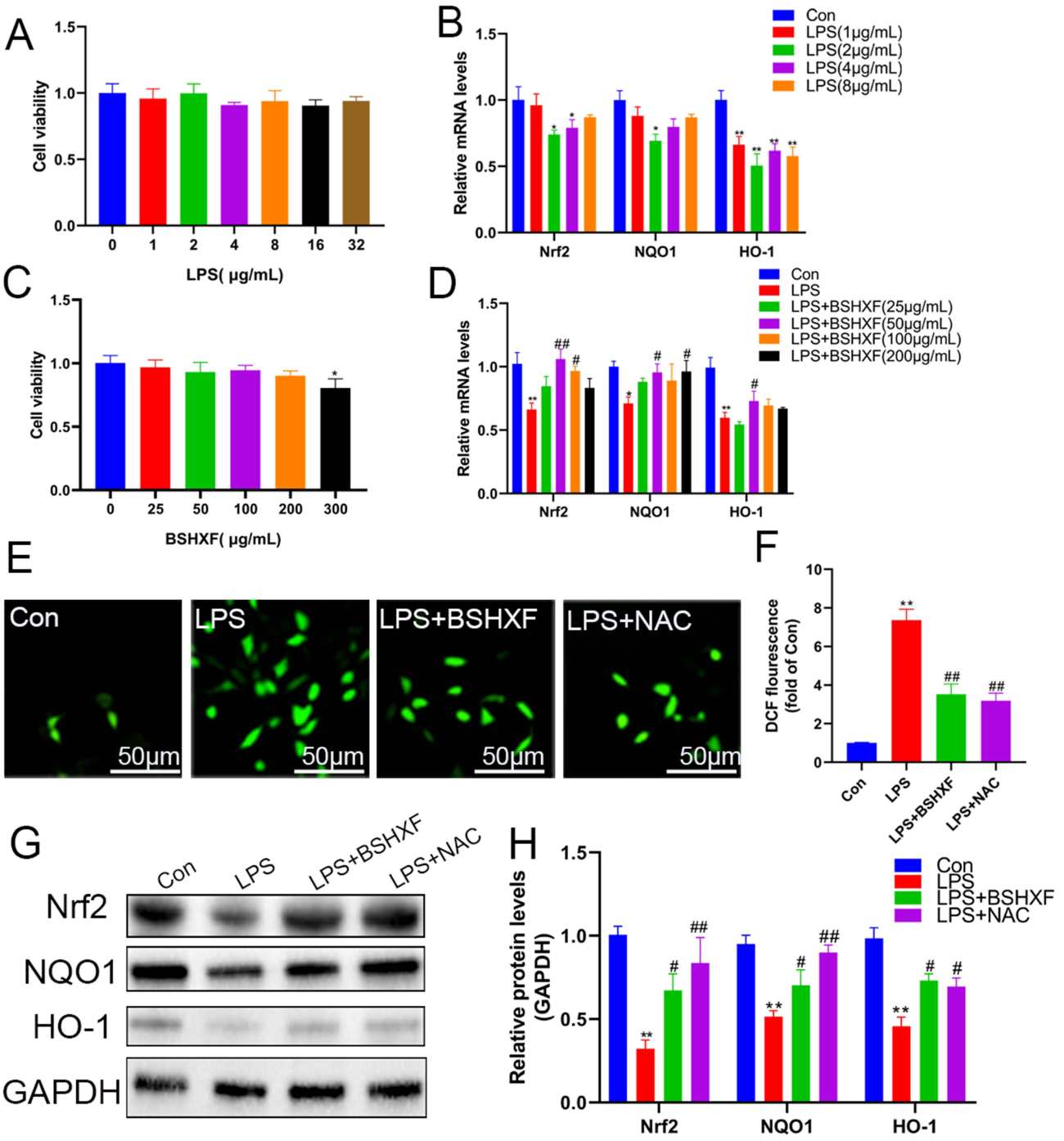

Figure 8 BSHXF effectively eliminated reactive oxygen species and activated the Nrf2 pathway. (**A**)Cell viability of neurons treated with different concentrations of LPS. (**B**) Relative mRNA expression levels of Nrf2, NQO1, and HO-1 in neurons exposed to different doses of LPS. (**C**) Cell viability following treatment with different concentrations of BSHXF. (**D**) Optimal concentration of BSHXF determined by measuring mRNA levels of antioxidant genes (Nrf2, NQO1, and HO-1) in neurons. (**E**) Measurement of reactive oxygen species levels induced by LPS, assessed using H2DCF-DA. (**F**) Quantitative analysis of the fluorescent intensity of DCF. (**G**) Western blot analysis of the expression levels of Nrf2, HO-1, and NQO1. (**H**) Quantification of the relative protein levels for Nrf2, HO-1, and NQO1. Data are presented as means ± SEM. *p < 0.05 and **p < 0.01 compared with the Con group; $^{\#}$p < 0.05 and $^{\#\#}$p < 0.01 compared with the LPS group.

recommends formulations that tonify the kidneys and activate blood flow to treat SCI. In this study, we found that the formulation BSHXF protected spinal cord neurons against oxidative damage and apoptosis after injury and aided in functional recovery by activating the Nrf2-dependent antioxidant pathway.

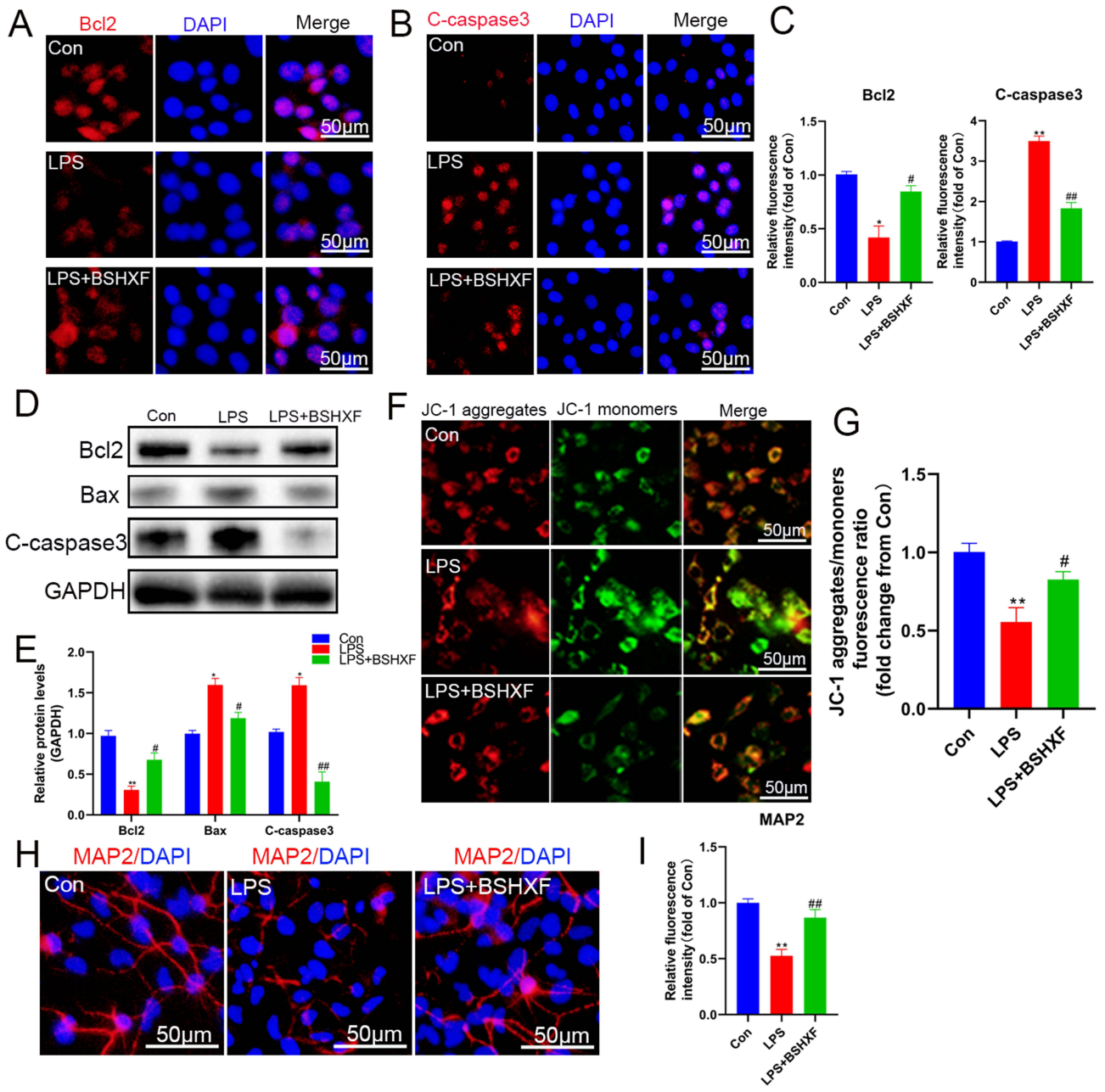

Figure 9 BSHXF mitigated LPS-induced apoptosis and axonal degeneration in neurons. (**A** and **B**) Fluorescence images showing the localization of Bcl2 and C-caspase3. (**C**) Quantification of fluorescence intensity for Bcl2 and C-caspase3. (**D**) Western blot analysis of C-caspase3, Bcl2, and Bax protein expression. (**E**) Quantification of the bands from Western blot analysis. (**F**) Mitochondrial membrane potential levels detected by JC-1 staining. (**G**) Ratios of polymeric (red) and monomeric (green) forms of JC-1, reflecting MMP in the indicated groups. (**H**) MAP2 visualized by fluorescein isothiocyanate fluorescence (red), with nuclei counterstained by DAPI (blue). (**I**) Statistical results of MAP2 fluorescence intensity across the groups. Data are presented as means ± SEM. *$p < 0.05$ and **$p < 0.01$ compared with the Con group; $^{\#}p < 0.05$ and $^{\#\#}p < 0.01$ compared with the LPS group.

We characterized the chemical components of BSHXF using HPLC. The main compounds identified included taurochenodeoxycholic acid, salvianic acid A, chlorogenic acid, paeoniflorin, polydatin, salvianolic acid B, salvianolic acid A, and mesaconitine. Multiple studies have reported the neuroprotective effects of these bioactive compounds in various neurological diseases. For instance, chlorogenic acid protects against neurological degeneration associated with oxidative stress in the brain.[33] Paeoniflorin has been shown to upregulate monoaminergic neurotransmitter levels and inhibit hypothalamic-pituitary-adrenal axis hyperactivity, promoting neuroprotection and facilitating hippocampal neurogenesis.[34] We have previously confirmed the neuro-regenerative effect of polydatin on SCI, and there is ample

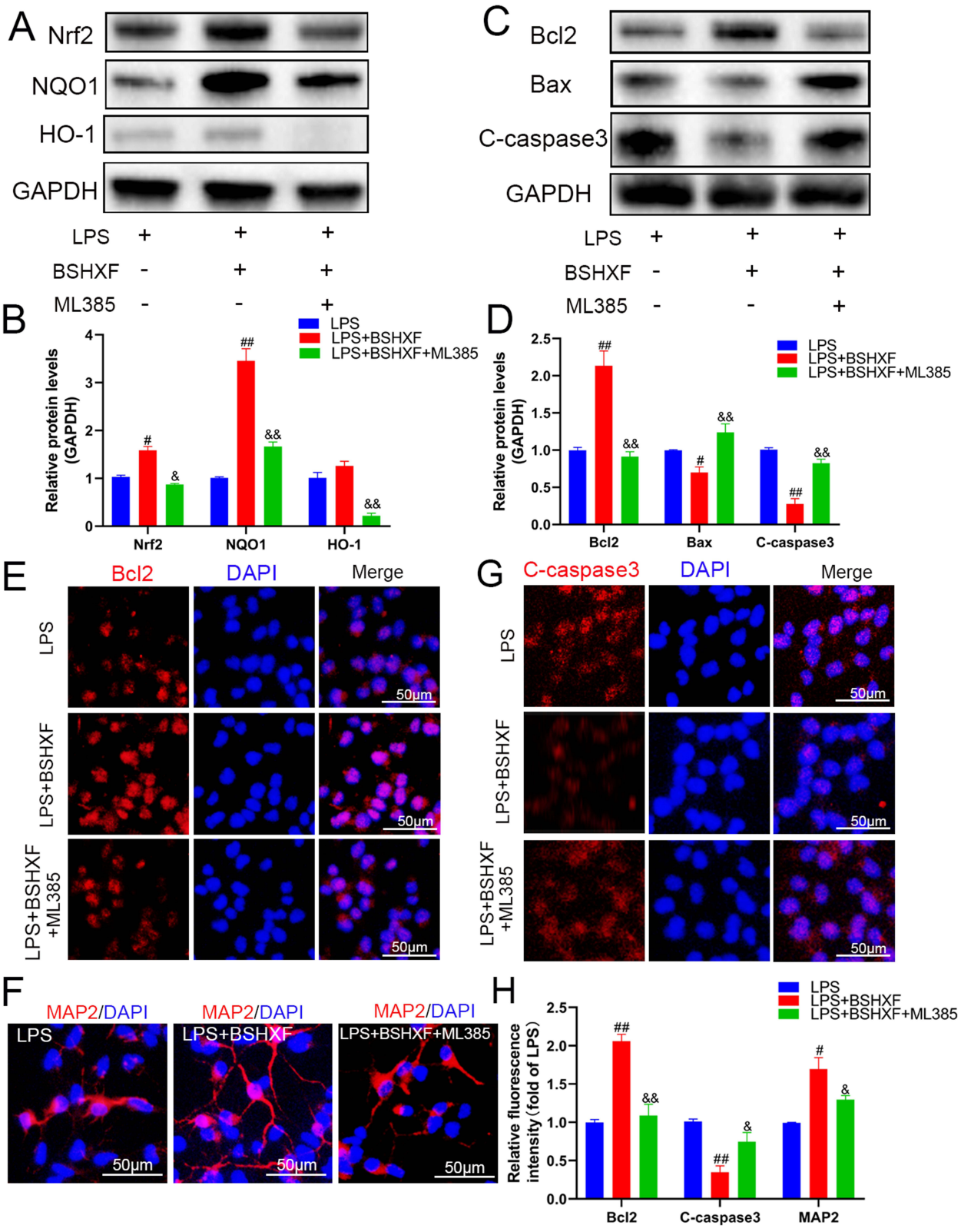

Figure 10 BSHXF reduced neuronal damage caused by oxidative stress by activating the Nrf2 pathway. (**A**) Western blot analysis of the expression of Nrf2 pathway-related proteins, including (Nrf2,NQO1, and HO-1). (**B**) Quantification of the bands from the Western blot analysis. (**C**) Western blot analysis of apoptotic proteins, including C-caspase3, Bcl2, and Bax. (**D**) Quantification of the bands from the Western blot analysis. (**E**) Immunofluorescence images showing Bcl2 expression in neurons. (**F**) Immunofluorescence images showing C-caspase3 expression in neurons. (**G**) Immunofluorescence images showing MAP2 expression in neurons. (**H**) Statistical chart of fluorescence signals. Data are presented as means ± SEM. $^{\#}p < 0.05$ and $^{\#\#}p < 0.01$ compared with the LPS group; $^{\&}p < 0.05$ and $^{\&\&}p < 0.01$ compared with the BSHXF group.

evidence of the neuroprotective effects of salvianolic acids against cerebral ischemia/reperfusion injury.[35–37] Nevertheless, the exact mechanisms through which these bioactive compounds exert their synergistic neuroprotective effects against SCI remain unclear.

BSHXF promoted motor function recovery in mice following SCI, as indicated by improved scores in behavioral tests. This improvement coincided with a significant reduction in lesion size and an increase in the number of mature neurons and Nissl bodies at the injury site in the BSHXF-treated mice. SCI triggers oxidative stress in the tissue, which can lead to neuronal apoptosis and exacerbate secondary injury. Thus, controlling secondary injury in the spinal cord can effectively reduce the risk of further neurological damage and enhance functional recovery.[38,39] In our study, levels of MDA and SOD were altered following SCI; however, BSHXF treatment decreased MDA levels and increased SOD activity. In the acute stage of SCI, Nrf2 pathway proteins (Nrf2, HO-1, NQO1) were significantly downregulated but recovered to varying degrees after 3 and 7 days of BSHXF administration. These results suggest that the inhibition of oxidative stress by BSHXF may relate to the activation of the Nrf2 pathway. Spinal cord lesions showed an increase in Tunel-positive cells, alongside upregulation of Bax and downregulation of Bcl2. However, treatment with BSHXF mitigated apoptosis and reversed the changes in apoptosis-related proteins. In addition to neuronal loss, SCI is characterized by axonal degeneration and demyelination, which can worsen the secondary injury response, leading to neural dysfunction and further symptom exacerbation. Therefore, the aim of SCI treatment is to protect neurons, promote remyelination, and reduce glial scar formation. As expected, SCI resulted in extensive glial scarring and severe neuronal loss at the injury site, which was alleviated and restored by BSHXF treatment. Oligodendrocyte death due to SCI can lead to demyelination and subsequent axonal damage. We found that BSHXF treatment counteracted myelin and axonal loss following SCI, and increased GAP43-positive axons and MBP-positive myelin. BSHXF exerted neuroprotective effects after SCI by inhibiting oxidative stress and alleviating neuronal apoptosis via the activation of the Nrf2 signaling pathway.

BSHXF also protected primary neurons against LPS-induced oxidative stress and apoptosis. LPS can induce oxidative stress, leading to neuronal apoptosis and axonal damage. BSHXF intervention reduced the incidence of oxidative stress, neuronal apoptosis, and axonal degeneration. However, the effect of BSHXF was significantly weakened when given concurrently with Nrf2 pathway inhibitors. Thus, BSHXF protects neurons by activating the Nrf2 pathway.

Conclusion

In conclusion, BSHXF promoted neurological recovery in mice with SCI by inhibiting oxidative stress and apoptosis in affected neurons, which reduced the scar area and neuronal loss, inhibited axonal degeneration, and promoted remyelination. The therapeutic effects of BSHXF were mediated through the Nrf2 signaling pathway, making BSHXF an effective therapeutic intervention for the postoperative rehabilitation of patients with spinal cord injuries.

Data Sharing Statement

The data used to support the findings of this study are included within the article.

Funding

This study was financially supported by National Natural Science Foundation of China (No. 82074451),the Research Project of Traditional Chinese Medicine Bureau of Guangdong Province (No. 20221178),the National Natural Science Foundation of China Youth Fund (No. 82104895),the Science and Technology Program of Guangzhou (No. 202201010974, and No. 202102010203) and the China Postdoctoral Science Foundation (No. 2021M700905).

Disclosure

The authors report no conflicts of interest in this work.

References

1. Anjum A, Yazid MD, Fauzi DM. et al. Spinal cord injury: pathophysiology, multimolecular interactions, and underlying recovery mechanisms. *Int J Mol Sci*. 2020;21(20):7533. doi:10.3390/ijms21207533

2. Palumbo ML, Moroni AD, Quiroga S, Castro MM, Burgueno AL, Genaro AM. Immunomodulation induced by central nervous system-related peptides as a therapeutic strategy for neurodegenerative disorders. *Pharmacol Res Perspect*. 2021;9(5):e00795. doi:10.1002/prp2.795
3. Peng W, Wan L, Luo Z, et al. Microglia-derived exosomes improve spinal cord functional recovery after injury via inhibiting oxidative stress and promoting the survival and function of endothelia cells. *Oxid Med Cell Longev*. 2021;2021(1):1695087. doi:10.1155/2021/1695087
4. Wang SY, Hong SR, Tan JY. Five different lives after suffering from spinal cord injury: the experiences of nurses who take care of spinal cord injury patients. *Int J Environ Res Public Health*. 2022;19(3). doi:10.3390/ijerph19031058
5. Thomas GS, Oliver DS, Romeo CC. Spinal cord injury management based on microglia-targeting therapies. *J Clin Med*. 2024;13(10):2773. doi:10.3390/jcm13102773
6. Hosseini SM, Borys B, Karimi-Abdolrezaee S. Neural stem cell therapies for spinal cord injury repair: an update on recent preclinical and clinical advances. *Brain*. 2024;147(3):766–793. doi:10.1093/brain/awad392
7. Hu X, Xu W, Ren Y, et al. Spinal cord injury: molecular mechanisms and therapeutic interventions. *Signal Transduct Target Ther*. 2023;8(1):245. doi:10.1038/s41392-023-01477-6
8. Rodrigues LF, Moura-Neto V, e Spohr TC. Biomarkers in spinal cord injury: from prognosis to treatment. *Mol Neurobiol*. 2018;55(8):6436–6448. doi:10.1007/s12035-017-0858-y
9. Sterner RC, Sterner RM. Immune response following traumatic spinal cord injury: pathophysiology and therapies. *Front Immunol*. 2022;13:1084101. doi:10.3389/fimmu.2022.1084101
10. Tian T, Zhang S, Yang M. Recent progress and challenges in the treatment of spinal cord injury. *Protein Cell*. 2023;14(9):635–652. doi:10.1093/procel/pwad003
11. Li J, Luo W, Xiao C, et al. Recent advances in endogenous neural stem/progenitor cell manipulation for spinal cord injury repair. *Theranostics*. 2023;13(12):3966–3987. doi:10.7150/thno.84133
12. Quadri SA, Farooqui M, Ikram A, et al. Recent update on basic mechanisms of spinal cord injury. *Neurosurg Rev*. 2020;43(2):425–441. doi:10.1007/s10143-018-1008-3
13. Adegeest CY, Ter Wengel PV, Peul WC. Traumatic spinal cord injury: acute phase treatment in critical care. *Curr Opin Crit Care*. 2023;29(6):659–665. doi:10.1097/MCC.0000000000001110
14. Lin QB, Chen P, Liu Y, Li N. Effects of tonifying kidney and blood circulation soup on the expression of Tau protein and neurotrophic factor in rats with spinal cord injury. *J Hunan Univ Trad Chin Med*. 2021;41:1851–1856. Chinese.
15. Wei YM. Zhou MT.esearch progress on modernized treatment of spinal cord injury in traditional Chinese medicine. *China Modern Med*. 2024;31(13):175–179. Chinese.
16. Hou Y, Luo D, Hou Y, et al. Bu Shen Huo Xue decoction promotes functional recovery in spinal cord injury mice by improving the microenvironment to promote axonal regeneration. *Chin Med*. 2022;17(1):85. doi:10.1186/s13020-022-00639-y
17. Wang SF, Zhang XR, Zhang HB. Study on the effect of tonifying the kidney and activating blood circulation soup plus reduction and acupuncture combined with hyperbaric oxygen on the rehabilitation of patients with spinal fracture and spinal cord injury after surgery. *World TCM*. 2019;14:3040–3044. Chinese.
18. Zhan J, Li X, Luo D, et al. Polydatin promotes the neuronal differentiation of bone marrow mesenchymal stem cells in vitro and in vivo: involvement of Nrf2 signalling pathway. *J Cell Mol Med*. 2020;24(9):5317–5329. doi:10.1111/jcmm.15187
19. Chen S, Tian R, Luo D, Xiao Z, Li H, Lin D. Time-course changes and role of autophagy in primary spinal motor neurons subjected to oxygen-glucose deprivation: insights into autophagy changes in a cellular model of spinal cord ischemia. *Front Cell Neurosci*. 2020;14:38. doi:10.3389/fncel.2020.00038
20. Qi YC, Duan GZ, Mao W, Liu Q, Zhang YL, Li PF. Taurochenodeoxycholic acid mediates cAMP-PKA-CREB signaling pathway. *Chin J Nat Med*. 2020;18(12):898–906. doi:10.1016/S1875-5364(20)60033-4
21. Li L, Liu Y, Zhao X, et al. Salvianic acid A sodium promotes the recovery of motor function after spinal cord injury in rats by reducing microglia inflammation through regulating MIP2/Vdac1/Ndufa12 signaling axis. *Orthop Surg*. 2020;12(6):1971–1979. doi:10.1111/os.12808
22. Miao M, Xiang L. Pharmacological action and potential targets of chlorogenic acid. *Adv Pharmacol*. 2020;87:71–88. doi:10.1016/bs.apha.2019.12.002
23. Zhang L, Wei W. Anti-inflammatory and immunoregulatory effects of paeoniflorin and total glucosides of paeony. *Pharmacol Ther*. 2020;207:107452. doi:10.1016/j.pharmthera.2019.107452
24. Lv R, Du L, Zhang L, Zhang Z. Polydatin attenuates spinal cord injury in rats by inhibiting oxidative stress and microglia apoptosis via Nrf2/HO-1 pathway. *Life Sci*. 2019;217:119–127. doi:10.1016/j.lfs.2018.11.053
25. Xiao Z, Liu W, Mu YP, et al. Pharmacological effects of salvianolic acid B against oxidative damage. *Front Pharmacol*. 2020;11:572373. doi:10.3389/fphar.2020.572373
26. Zhang HF, Wang JH, Wang YL, et al. Salvianolic acid A protects the kidney against oxidative stress by activating the Akt/GSK-3beta/Nrf2 signaling pathway and inhibiting the NF-kappaB signaling pathway in 5/6 nephrectomized rats. *Oxid Med Cell Longev*. 2019;2019:2853534. doi:10.1155/2019/2853534
27. Sun Z, Yang L, Zhao L, Cui R, Yang W. Neuropharmacological effects of mesaconitine: evidence from molecular and cellular basis of neural circuit. *Neural Plast*. 2020;2020:8814531. doi:10.1155/2020/8814531
28. Liu Z, Yao X, Jiang W, et al. Advanced oxidation protein products induce microglia-mediated neuroinflammation via MAPKs-NF-kappaB signaling pathway and pyroptosis after secondary spinal cord injury. *J Neuroinflammation*. 2020;17(1):90. doi:10.1186/s12974-020-01751-2
29. Chen J, Shen Y, Shao X, Wu W. An emerging role of inflammasomes in spinal cord injury and spinal cord tumor. *Front Immunol*. 2023;14:1119591. doi:10.3389/fimmu.2023.1119591
30. Feigin VL, Nichols E, Alam T, et al. Global, regional, and national burden of neurological disorders, 1990–2016: a systematic analysis for the global burden of disease study 2016. *Lancet Neurol*. 2019;18(5):459–480. doi:10.1016/S1474-4422(18)30499-X
31. Wang L, Gu X. Prof. Gu Xizhen's experience in treating spinal cord injuries from the theory of "deficiency and cold of kidney governor". *Chin Med Inf*. 2019;36:70–72. Chinese.
32. He F, Mu X, Fu L, et al. Current status of Chinese medicine research on spinal cord injury. *World J Integr Med*. 2017;12:440–444. Chinese.
33. Heitman E, Ingram DK. Cognitive and neuroprotective effects of chlorogenic acid. *Nutr Neurosci*. 2017;20(1):32–39. doi:10.1179/1476830514Y.0000000146

34. Wang XL, Feng ST, Wang YT, Chen NH, Wang ZZ, Zhang Y. Paeoniflorin: a neuroprotective monoterpenoid glycoside with promising anti-depressive properties. *Phytomedicine*. 2021;90:153669. doi:10.1016/j.phymed.2021.153669
35. Hou S, Zhao MM, Shen PP, Liu XP, Sun Y, Feng JC. Neuroprotective effect of salvianolic acids against cerebral ischemia/reperfusion injury. *Int J Mol Sci*. 2016;17(7):1190. doi:10.3390/ijms17071190
36. Xu S, Zhong A, Ma H, et al. Neuroprotective effect of salvianolic acid B against cerebral ischemic injury in rats via the CD40/NF-kappaB pathway associated with suppression of platelets activation and neuroinflammation. *Brain Res*. 2017;1661:37–48. doi:10.1016/j.brainres.2017.02.011
37. Ma DC, Zhang NN, Zhang YN, Chen HS. Salvianolic acids for injection alleviates cerebral ischemia/reperfusion injury by switching M1/M2 phenotypes and inhibiting NLRP3 inflammasome/pyroptosis axis in microglia in vivo and in vitro. *J Ethnopharmacol*. 2021;270:113776. doi:10.1016/j.jep.2021.113776
38. Liu X, Zhang Y, Wang Y, Qian T. Inflammatory response to spinal cord injury and its treatment. *World Neurosurg*. 2021;155:19–31. doi:10.1016/j.wneu.2021.07.148
39. Kong X, Gao J. Macrophage polarization: a key event in the secondary phase of acute spinal cord injury. *J Cell Mol Med*. 2017;21(5):941–954. doi:10.1111/jcmm.13034